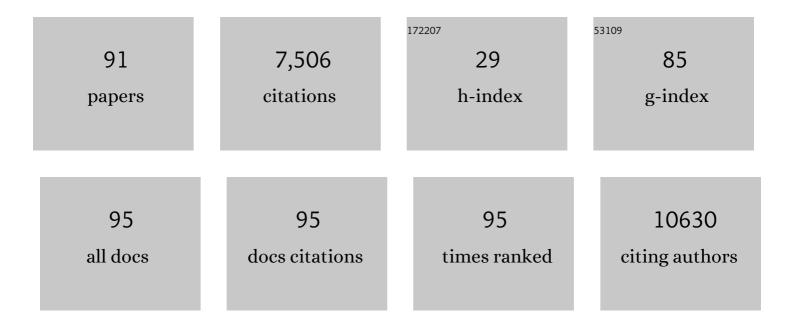
List of Publications by Year in descending order

Source: https://exaly.com/author-pdf/5436292/publications.pdf Version: 2024-02-01



KENNETH W FISHBEIN

#	Article	IF	CITATIONS
1	ATP synthase K+- and H+-fluxes drive ATP synthesis and enable mitochondrial K+-"uniporter―function: II. Ion and ATP synthase flux regulation. Function, 2022, 3, zqac001.	1.1	20
2	Muscle mitochondrial energetics predicts mobility decline in wellâ€functioning older adults: The baltimore longitudinal study of aging. Aging Cell, 2022, 21, e13552.	3.0	32
3	ATP Synthase K+- and H+-Fluxes Drive ATP Synthesis and Enable Mitochondrial K+-"Uniporter― Function: I. Characterization of Ion Fluxes. Function, 2022, 3, zqab065.	1.1	25
4	Ankleâ€Brachial Index and Energy Production in People Without Peripheral Artery Disease: The BLSA. Journal of the American Heart Association, 2022, 11, e019014.	1.6	2
5	Stabilization of parameter estimates from multiexponential decay through extension into higher dimensions. Scientific Reports, 2022, 12, 5773.	1.6	5
6	Designer Receptors Exclusively Activated by Designer Drugs Approach to Treatment of Sleep-disordered Breathing. American Journal of Respiratory and Critical Care Medicine, 2021, 203, 102-110.	2.5	25
7	Cardiovascular Health and Mitochondrial Function: Testing an Association. Journals of Gerontology - Series A Biological Sciences and Medical Sciences, 2021, 76, 361-367.	1.7	10
8	A cross-sectional study of functional and metabolic changes during aging through the lifespan in male mice. ELife, 2021, 10, .	2.8	47
9	Association of central arterial stiffness with hippocampal blood flow and N-acetyl aspartate concentration in hypertensive adult Dahl salt sensitive rats. Journal of Hypertension, 2021, 39, 2113-2121.	0.3	1
10	Contribution of Intramyocellular Lipids to Decreased Computed Tomography Muscle Density With Age. Frontiers in Physiology, 2021, 12, 632642.	1.3	3
11	Mitochondrial DNA copy number and heteroplasmy load correlate with skeletal muscle oxidative capacity by P31 MR spectroscopy. Aging Cell, 2021, 20, e13487.	3.0	8
12	Disulfiram Treatment Normalizes Body Weight in Obese Mice. Cell Metabolism, 2020, 32, 203-214.e4.	7.2	46
13	Poor mitochondrial health and systemic inflammation? Test of a classic hypothesis in the Baltimore Longitudinal Study of Aging. GeroScience, 2020, 42, 1175-1182.	2.1	23
14	Topoisomerase 3Î <sup>2</sup> knockout mice show transcriptional and behavioural impairments associated with neurogenesis and synaptic plasticity. Nature Communications, 2020, 11, 3143.	5.8	22
15	Proteomic signatures of in vivo muscle oxidative capacity in healthy adults. Aging Cell, 2020, 19, e13124.	3.0	13
16	Greater Skeletal Muscle Oxidative Capacity Is Associated With Higher Resting Metabolic Rate: Results From the Baltimore Longitudinal Study of Aging. Journals of Gerontology - Series A Biological Sciences and Medical Sciences, 2020, 75, 2262-2268.	1.7	18
17	Effects of Lisinopril on Arterial Stiffness, Cerebral Blood Flow and Cortical Thickness in Hypertensive Dahlâ€6 Rats. FASEB Journal, 2020, 34, 1-1.	0.2	0
18	Effects of Lisinopril on Arterial Stiffness, Cerebral Blood Flow, Neuronal Viability and Cortical Thickness in Lateâ€Life Hypertension in Dahlâ€S Rats. FASEB Journal, 2020, 34, 1-1.	0.2	0

#	Article	IF	CITATIONS
19	Targeted Retrograde Chemogenetic Approach to Treat Sleep Apnea. FASEB Journal, 2020, 34, 1-1.	0.2	0
20	Stabilization of T <sub>2</sub> relaxation and magnetization transfer in cartilage explants by immersion in perfluorocarbon liquid. Magnetic Resonance in Medicine, 2019, 81, 3209-3217.	1.9	3
21	Low plasma lysophosphatidylcholines are associated with impaired mitochondrial oxidative capacity in adults in the Baltimore Longitudinal Study of Aging. Aging Cell, 2019, 18, e12915.	3.0	34
22	Moderateâ€ŧoâ€Vigorous Physical Activity Is Associated With Higher Muscle Oxidative Capacity in Older Adults. Journal of the American Geriatrics Society, 2019, 67, 1695-1699.	1.3	27
23	The Role of Muscle Perfusion in the Age-Associated Decline of Mitochondrial Function in Healthy Individuals. Frontiers in Physiology, 2019, 10, 427.	1.3	31
24	Diffusionâ€weighted MRI with intravoxel incoherent motion modeling for assessment of muscle perfusion in the thigh during postâ€exercise hyperemia in younger and older adults. NMR in Biomedicine, 2019, 32, e4072.	1.6	17
25	Age and Muscle Function Are More Closely Associated With Intracellular Magnesium, as Assessed by 31P Magnetic Resonance Spectroscopy, Than With Serum Magnesium. Frontiers in Physiology, 2019, 10, 1454.	1.3	14
26	A Novel Extension to Fuzzy Connectivity for Body Composition Analysis: Applications in Thigh, Brain, and Whole Body Tissue Segmentation. IEEE Transactions on Biomedical Engineering, 2019, 66, 1069-1081.	2.5	12
27	Screening of ligands for redox-active europium using magnetic resonance imaging. Bioorganic and Medicinal Chemistry, 2018, 26, 5274-5279.	1.4	7
28	Measurement of fat fraction in the human thymus by localized NMR and three-point Dixon MRI techniques. Magnetic Resonance Imaging, 2018, 50, 110-118.	1.0	4
29	Overexpression of <scp>CYB</scp> 5R3 and <scp>NQO</scp> 1, two <scp>NAD</scp> <sup>+</sup> â€producing enzymes, mimics aspects of caloric restriction. Aging Cell, 2018, 17, e12767.	3.0	32
30	Muscle strength mediates the relationship between mitochondrial energetics and walking performance. Aging Cell, 2017, 16, 461-468.	3.0	99
31	The effect of noise and lipid signals on determination of Gaussian and nonâ€Gaussian diffusion parameters in skeletal muscle. NMR in Biomedicine, 2017, 30, e3718.	1.6	15
32	Chemogenetic stimulation of the hypoglossal neurons improves upper airway patency. Scientific Reports, 2017, 7, 44392.	1.6	35
33	Lower Mitochondrial Energy Production of the Thigh Muscles in Patients With Lowâ€Normal Ankleâ€Brachial Index. Journal of the American Heart Association, 2017, 6, .	1.6	23
34	Activatable interpolymer complex-superparamagnetic iron oxide nanoparticles as magnetic resonance contrast agents sensitive to oxidative stress. Colloids and Surfaces B: Biointerfaces, 2017, 158, 578-588.	2.5	18
35	Insulin Resistance Is Associated With Reduced Mitochondrial Oxidative Capacity Measured by 31P-Magnetic Resonance Spectroscopy in Participants Without Diabetes From the Baltimore Longitudinal Study of Aging. Diabetes, 2017, 66, 170-176.	0.3	48
36	Multiparametric Classification of Skin from Osteogenesis Imperfecta Patients and Controls by Quantitative Magnetic Resonance Microimaging. PLoS ONE, 2016, 11, e0157891.	1.1	4

#	Article	IF	CITATIONS
37	Analysis of mcDESPOT―and CPMGâ€derived parameter estimates for twoâ€component nonexchanging systems. Magnetic Resonance in Medicine, 2016, 75, 2406-2420.	1.9	40
38	Cytochrome b5 reductase and the control of lipid metabolism and healthspan. Npj Aging and Mechanisms of Disease, 2016, 2, 16006.	4.5	57
39	<sup>31</sup> P Magnetic Resonance Spectroscopy Assessment of Muscle Bioenergetics as a Predictor of Gait Speed in the Baltimore Longitudinal Study of Aging. Journals of Gerontology - Series A Biological Sciences and Medical Sciences, 2016, 71, 1638-1645.	1.7	80
40	Aortic Fibrosis, Induced by High Salt Intake in the Absence of Hypertensive Response, Is Reduced by a Monoclonal Antibody to Marinobufagenin. American Journal of Hypertension, 2016, 29, 641-646.	1.0	22
41	Sensitivity and specificity of univariate MRI analysis of experimentally degraded cartilage under clinical imaging conditions. Journal of Magnetic Resonance Imaging, 2015, 42, 136-144.	1.9	8
42	Incorporation of rician noise in the analysis of biexponential transverse relaxation in cartilage using a multiple gradient echo sequence at 3 and 7 tesla. Magnetic Resonance in Medicine, 2015, 73, 352-366.	1.9	37
43	Classification of histologically scored human knee osteochondral plugs by quantitative analysis of magnetic resonance images at 3T. Journal of Orthopaedic Research, 2015, 33, 640-650.	1.2	13
44	Combination therapy with lenalidomide and nanoceria ameliorates CNS autoimmunity. Experimental Neurology, 2015, 273, 151-160.	2.0	43
45	Image-based Tissue Distribution Modeling for Skeletal Muscle Quality Characterization. IEEE Transactions on Biomedical Engineering, 2015, 63, 1-1.	2.5	6
46	Adiposity induces lethal cytokine storm after systemic administration of stimulatory immunotherapy regimens in aged mice. Journal of Experimental Medicine, 2014, 211, 2373-2383.	4.2	124
47	Metabolic abnormalities and hypoleptinemia in α-synuclein A53T mutant mice. Neurobiology of Aging, 2014, 35, 1153-1161.	1.5	23
48	Adiposity As a Principal Component of Lethal Cytokine Storm Following Cancer Immunotherapy in Aged Mice. Blood, 2014, 124, 460-460.	0.6	1
49	Stabilization of the inverse Laplace transform of multiexponential decay through introduction of a second dimension. Journal of Magnetic Resonance, 2013, 236, 134-139.	1.2	33
50	Characterization of Engineered Cartilage Constructs Using Multiexponential <i>T</i> <sub>2</sub> Relaxation Analysis and Support Vector Regression. Tissue Engineering - Part C: Methods, 2012, 18, 433-443.	1.1	15
51	Automated quantification of muscle and fat in the thigh from waterâ€, fatâ€, and nonsuppressed MR images. Journal of Magnetic Resonance Imaging, 2012, 35, 1152-1161.	1.9	37
52	Multivariate analysis of cartilage degradation using the support vector machine algorithm. Magnetic Resonance in Medicine, 2012, 67, 1815-1826.	1.9	31
53	Characterization of skin abnormalities in a mouse model of osteogenesis imperfecta using high resolution magnetic resonance imaging and Fourier transform infrared imaging spectroscopy. NMR in Biomedicine, 2012, 25, 169-176.	1.6	11
54	Between a Rock and a Hard Place: Mitochondria Deform Anisotropically in Intact Cardiomyocytes During Active Contraction. Biophysical Journal, 2011, 100, 288a.	0.2	0

#	Article	IF	CITATIONS
55	Towards segmentation of the thymus in fat and water parametric MR images. , 2011, 2011, 8078-81.		О
56	XRCC1 haploinsufficiency in mice has little effect on aging, but adversely modifies exposure-dependent susceptibility. Nucleic Acids Research, 2011, 39, 7992-8004.	6.5	25
57	Cardiac phenotype induced by a dysfunctional α <sub>1C</sub> transgene. Channels, 2011, 5, 138-147.	1.5	2
58	Analysis of Mitochondrial 3D-Deformation in Cardiomyocytes during Active Contraction Reveals Passive Structural Anisotropy of Orthogonal Short Axes. PLoS ONE, 2011, 6, e21985.	1.1	34
59	Compatibility of superparamagnetic iron oxide nanoparticle labeling for <sup>1</sup> H MRI cell tracking with <sup>31</sup> P MRS for bioenergetic measurements. NMR in Biomedicine, 2010, 23, 1166-1172.	1.6	7
60	Characterization of <i>Ex Vivo</i> –Generated Bovine and Human Cartilage by Immunohistochemical, Biochemical, and Magnetic Resonance Imaging Analyses. Tissue Engineering - Part A, 2010, 16, 2183-2196.	1.6	18
61	Automated Quantification of Muscle and Fat in the Thigh from Water-, Fat- and Non-suppressed MR Images. , 2010, , .		Ο
62	Magnetic Resonance Imaging of Chondrocytes Labeled with Superparamagnetic Iron Oxide Nanoparticles in Tissue-Engineered Cartilage. Tissue Engineering - Part A, 2009, 15, 3899-3910.	1.6	67
63	Multicomponent T <sub>2</sub> relaxation analysis in cartilage. Magnetic Resonance in Medicine, 2009, 61, 803-809.	1.9	149
64	Assessment of tissue repair in full thickness chondral defects in the rabbit using magnetic resonance imaging transverse relaxation measurements. Journal of Biomedical Materials Research - Part B Applied Biomaterials, 2008, 86B, 375-380.	1.6	21
65	Noninvasive Assessment of Glycosaminoglycan Production in Injectable Tissue-Engineered Cartilage Constructs Using Magnetic Resonance Imaging. Tissue Engineering - Part C: Methods, 2008, 14, 243-249.	1.1	25
66	Cryopreservation of porcine articular cartilage: MRI and biochemical results after different freezing protocols. Cryobiology, 2007, 54, 36-43.	0.3	28
67	Optimal methods for the preservation of cartilage samples in MRI and correlative biochemical studies. Magnetic Resonance in Medicine, 2007, 57, 866-873.	1.9	25
68	Effects of formalin fixation and collagen cross-linking onT2 and magnetization transfer in bovine nasal cartilage. Magnetic Resonance in Medicine, 2007, 57, 1000-1011.	1.9	65
69	Effects of knee injection on skeletal muscle metabolism and contractile force in rats. Osteoarthritis and Cartilage, 2007, 15, 550-558.	0.6	3
70	Fourier transform infrared imaging and MR microscopy studies detect compositional and structural changes in cartilage in a rabbit model of osteoarthritis. Analytical and Bioanalytical Chemistry, 2007, 387, 1601-1612.	1.9	69
71	Development of cardiomyopathy in response to chronic βâ€adrenegric stimulation of transgenic mouse overexpressing the exonâ€22 isoform of the human Ca <sub>v</sub> 1.2 channel <sub>α1C</sub> subunit as revealed by magnetic resonance imaging. FASEB Journal, 2007, 21, A583.	0.2	0
72	Resveratrol improves health and survival of mice on a high-calorie diet. Nature, 2006, 444, 337-342.	13.7	3,882

#	Article	IF	CITATIONS
73	Compatibility of Gd-DTPA perfusion and histologic studies of the brain. Magnetic Resonance Imaging, 2006, 24, 27-31.	1.0	14
74	An analysis of the integration between articular cartilage and nondegradable hydrogel using magnetic resonance imaging. Journal of Biomedical Materials Research - Part B Applied Biomaterials, 2006, 77B, 144-148.	1.6	40
75	Tendon and neurovascular bundle displacement in the palm with hand flexion and extension: An MRI and gross anatomy correlative study. Journal of Magnetic Resonance Imaging, 2006, 23, 742-746.	1.9	3
76	Glycogen synthase kinase-3Î <sup>2</sup> mediates convergence of protection signaling to inhibit the mitochondrial permeability transition pore. Journal of Clinical Investigation, 2004, 113, 1535-1549.	3.9	854
77	Ex vivo magnetic resonance microscopy of an osteochondral transfer. Journal of Magnetic Resonance Imaging, 2003, 17, 603-608.	1.9	22
78	Matrix fixed-charge density as determined by magnetic resonance microscopy of bioreactor-derived hyaline cartilage correlates with biochemical and biomechanical properties. Arthritis and Rheumatism, 2003, 48, 1047-1056.	6.7	69
79	Differences in the Bioenergetic Response of the Isolated Perfused Rat Heart to Selective β1- and β2-Adrenergic Receptor Stimulation. Circulation, 2003, 107, 2146-2152.	1.6	10
80	A central nervous system specific mouse model for thanatophoric dysplasia type II. Human Molecular Genetics, 2003, 12, 2863-2871.	1.4	30
81	The lever-coil: a simple, inexpensive sensor for respiratory and cardiac motion in MRI experiments. Magnetic Resonance Imaging, 2001, 19, 881-889.	1.0	26
82	Pitfalls in the Measurement of Metabolite Concentrations Using the One-Pulse Experiment in in Vivo NMR: Commentary on "On Neglecting Chemical Exchange Effects When Correcting in Vivo31P MRS Data for Partial Saturation― Journal of Magnetic Resonance, 2001, 149, 251-257.	1.2	12
83	Measurement of Spin–Lattice Relaxation Times and Concentrations in Systems with Chemical Exchange Using the One-Pulse Sequence: Breakdown of the Ernst Model for Partial Saturation in Nuclear Magnetic Resonance Spectroscopy. Journal of Magnetic Resonance, 2000, 142, 120-135.	1.2	69
84	31P NMR spectroscopy of developing cartilage produced from chick chondrocytes in a hollow-fiber bioreactor. Magnetic Resonance in Medicine, 2000, 44, 367-372.	1.9	18
85	Adenovirus-Mediated VEGF <sub>121</sub> Gene Transfer Stimulates Angiogenesis in Normoperfused Skeletal Muscle and Preserves Tissue Perfusion After Induction of Ischemia. Circulation, 2000, 102, 565-571.	1.6	130
86	Cartilage formation in a hollow fiber bioreactor studied by proton magnetic resonance microscopy. Matrix Biology, 1998, 17, 513-523.	1.5	53
87	Bioreactor and probe system for magnetic resonance microimaging and spectroscopy of chondrocytes and neocartilage. International Journal of Imaging Systems and Technology, 1997, 8, 285-292.	2.7	19
88	A Spectrometer for Dynamic Nuclear Polarization and Electron Paramagnetic Resonance at High Frequencies. Journal of Magnetic Resonance Series A, 1995, 117, 28-40.	1.6	163
89	Rotational resonance with multipleâ€pulse scaling in solidâ€state nuclear magnetic resonance. Journal of Chemical Physics, 1994, 100, 5533-5545.	1.2	13
90	Two-dimensional solid-state proton NMR and proton exchange. Journal of the American Chemical Society, 1993, 115, 6254-6261.	6.6	80

#	Article	IF	CITATIONS
91	Pulsed dynamic nuclear polarization at 5 T. Chemical Physics Letters, 1992, 189, 54-59.	1.2	37